This is the Pre-Published Version.
The following publication H. Wang and I. W. -H. Ho, "CSI-based Passenger Counting on Public Transport Vehicles with Multiple Transceivers," 2024 IEEE Wireless Communications and Networking Conference (WCNC), Dubai, United Arab Emirates, 2024, pp. 1-6 is available at https://doi.org/10.1109/WCNC57260.2024.10571130.

CSI-based Passenger Counting on Public Transport Vehicles with Multiple Transceivers

He Wang, Ivan Wang-Hei Ho
Department of Electrical and Electronic Engineering
The Hong Kong Polytechnic University, Hong Kong
Email: edana.wang@connect.polyu.hk, ivanwh.ho@polyu.edu.hk

Abstract—**Wi-Fi sensing has enabled many applications due to the increasing number of commercial Wi-Fi devices and channel state information (CSI) extraction tools. In this paper, we study the application of CSI-based stationary crowd counting using multiple pairs of transceivers. Specifically, we provide an exact count of the number of passengers on the upper deck of a double-decker bus. Most of the previous solutions count the number of immobile people with a pair of transceivers, which leads to limited sensing scales with the maximum countable number achieved by the state-of-the-art solutions being 15. Indeed, few of these solutions consider the impact of the placement of transceivers on the sensing performance. The major innovation of our work is to identify the optimal topology for multiple receivers based on the Fresnel Zone model to improve the quality of data collection and reduce the overall training effort. We consider the impact of the First Fresnel Zone (FFZ) and the distance between transmitters and receivers when deploying multiple pairs of transceivers. This technique can also be applied to other applications, such as localization, tracking of multiple people, multi-person respiration rate monitoring, etc. The proposed topology was compared with a baseline of a pair of transceivers. Our results show that by properly placing transceivers, the accuracy of counting the exact number of passengers can be improved by more than 11.49%, and the sensing scalability can be extended from 11 to 20 passengers, with an average accuracy of 90.83% with conventional machine learning methods only.**

Index Terms—**Crowd counting, Passenger counting, Wi-Fi sensing, CSI, Multi-sensors, Fresnel Zone, Deployment.**

I. Introduction

Wi-Fi has become one of the most prominent wireless technologies, which is widely available in public areas and on common devices such as laptops, smartphones, etc. As a result, the growing importance and popularity of Wi-Fi sensing technology have triggered widespread interest among researchers in the wireless communication domain. Channel State Information (CSI) is one of the major types of data used in wireless sensing that can be extracted from Wi-Fi signals. CSI represents the communication channel between the transmitter (Tx) and the receiver (Rx) and contains information at the level of individual data subcarriers. Due to the release of CSI extraction tools [1], [2], CSI data is available and flexible for further processing, facilitating the development of CSI-based Wi-Fi sensing applications.

This work was supported in part by the Smart Traffic Fund (Project No. PSRI/31/2202/PR) established under the Transport Department of the Hong Kong Special Administrative Region (HKSAR), China.

One of the most important but challenging applications of Wi-Fi sensing is crowd-counting. CSI-based crowd counting outperforms traditional approaches such as video-based recognition and other non-image-based solutions like wearable sensors and radars in several aspects [3]–[6]. Most crowd-counting applications are achieved by computer vision techniques with images from cameras. Compared to camera-based approaches, CSI-based methods do not rely on the brightness of the surroundings and have non-line-of-sight (NLOS) capability. The second benefit of CSI-based methods over other solutions is their privacy-preserving nature. CSI-based methods use off-the-shelf Wi-Fi routers and are minimally intrusive to users. In addition, this method requires a relatively low cost because it does not need to install additional sensing infrastructure [7]. CSI-based methods also outperform other device-free crowd-counting approaches like received signal strength indicator (RSSI)-based methods as it is more sensitive to changes in the environment. CSI reveals information on the joint effect of scattering, fading, and power decay with distance, hence it is more suitable for indoor environments compared to the RSSI [7].

Previous research related to CSI-based crowd counting mostly focused on estimating the number of moving people in a meeting room, office, or laboratory [8]–[13], and participants in their studies were required to be in motion. Some of these studies have pointed out that they achieved low accuracy when a person was stationary. However, there are a great number of scenarios in which individuals are not moving around, such as readers in a library or passengers on public transportation. For public transportation, knowing the number of passengers or occupancy result is helpful for real-time adjustment of bus or subway schedules. Passengers can also determine their selections of compartments based on the number of available seats in the bus or subway. Nevertheless, it is a great challenge to count immobile people since there are fewer variations when people remain stationary. Wang et al. [14] proposed a system to count static users based on respiration tracking in a lab and a car with one Tx and one Rx. However, this system could only count up to four people and the accuracy of the crowd counting could be low when participants have the same respiration rates. Cheng et al. [15] proposed a counting system based on a deep neural network (DNN) model, which could count the exact number of the crowd up to nine with fixed positions. However, the accuracy of such deep-learning-based approaches is only maintained in the same environment and the same configuration. Jiang et al. [16] used a mathematical method to count up to 15 passengers based on the distribution of the weak fidgeting motion of passengers in a moving car or subway. The limitation of this method is that they cannot count a large number of passengers when at least one of the passengers is fidgeting all the time. The above studies show that it is difficult to count a large number of stationary people in an area. A possible solution addressed by [17] is to utilize more wireless links over large areas to count more people.

In this paper, we consider counting the number of passengers in a bus compartment with multiple links to increase the maximum countable number. In a wireless sensing system, the placement of sensors and the design of the sensing network can significantly affect the quality of the collected data. However, there is limited literature related to exploring the impact of the deployment of multiple sensors on wireless sensing. This paper attempts to pave the way in this important direction. We carefully consider the placement of sensors and network topology designs for optimal data collection and reducing the overall training effort. The line-of-sight (LOS) distance between the transmitter and the receiver has been proven to affect the sensing coverage significantly [18]. As the distance between the Tx and Rx increases, the sensing coverage area increases first, then decreases. If the placement is not carefully planned, the sensing coverage will be quite limited. In addition, the first fresnel zone (FFZ) of a wireless link will significantly affect the sensing ability of CSI-based applications [19], [20]. In this paper, we aim to jointly consider these factors and design a suitable topology for passenger counting on a double-decker bus.

The major contributions of this work are threefold:

- We have developed a prototype using commercial off-the-shelf Wi-Fi devices for passive passenger counting. Specifically, the Raspberry Pi installed with the Nexmon CSI Extraction Tool is used as the receiver. Previous works commonly use the laptop with the Intel 5300 network card, which only supports 30 subcarriers in 2.4 GHz. The Nexmon Tool is able to extract 242 subcarriers with 80 MHz bandwidth in 5 GHz, which provides more information. In fact, the Respiratory Pi is more suitable in real scenarios when compared to traditional laptops as it has a lower cost and smaller volume.
- We have proposed a topology with multiple sensors to increase the sensing coverage range. To the best of our knowledge, this is the first time that multiple sensors are applied for people-counting in the wireless sensing area. In addition, the deployment of Rx and Tx is considered with reference to the Fresnel Zone model to eliminate the negative effects due to diffracted signals. With the designed topology, we raise the measurement limit to 20 passengers.
- We have devised effective preprocessing methods that can remove noise and reduce the complexity of calculation for model training. We have applied an RSSI-based calculation to rescale the CSI amplitude and avoid the negative effect caused by the automatic gain control (AGC) in receivers. Principal component analysis (PCA) is applied to extract the characteristics of the data to the greatest scale and reduce the input size by at least 50.83%.

The rest of this paper is organized as follows. Section II introduces the fundamental technique and model of Wi-Fi-based sensing. The system designing procedure is described in Section III. Section IV presents the implementation and evaluation results of the passenger counting system. Section V discusses the conclusion and future works based on the findings in this paper.

II. Related Technical Theory Introduction

In this section, we introduce the basic knowledge and models of Wi-Fi sensing. Based on these theories, we design the topology that is applied to the crowd-counting system.

A. Channel State Information

In an indoor environment, radial signals can be reflected by many objects such as walls and human bodies, and thus arrive at a receiver through multiple paths. These paths can be classified into two types: static path and dynamic path. Static paths include the LOS path and the paths reflected from static objects. Dynamic paths are induced by changes in target objects, e.g., human motions. CSI is used to characterize the channel between a Tx and an Rx in Wi-Fi systems. The signal in the receiver can be expressed by (1), where $X(f,t)$ and $H(f,t)$ are the frequency domain representations of the transmitted signal and the complex-valued channel frequency response (CFR) at carrier frequency f and time t.

$$Y(f,t) = H(f,t) \times X(f,t) \tag{1}$$

Each CSI in the matrix can be represented as a linear superposition of all the paths as shown in (2), where H_s, H_d, and H_n represent the static path, dynamic path, and noise respectively. $|H|$ is the amplitude and θ is the phase of each CSI component.

$$\begin{aligned} H(f,t) &= H_s(f,t) + H_d(f,t) + H_n(f,t) \\ &= |H_s(f,t)|\, e^{-j\theta_s} + |H_d(f,t)|\, e^{-j\theta_d} \\ &+ |H_n(f,t)|\, e^{-j\theta_n} \end{aligned} \tag{2}$$

In an orthogonal frequency-division multiplexing (OFDM) system, the frequency space is separated into multiple subcarriers that are transmitted in parallel, i.e., the CSI will be different but correlated in subcarriers. Assuming N packets and S subcarriers are captured, the extracted CSI matrix can be written as (3), where $h_{i,j}$ represents the CSI values of the jth subcarrier at the ith packet.

$$H = \begin{bmatrix} h_{1,1} & h_{1,2} & \dots & h_{1,S} \\ h_{2,1} & h_{2,2} & \dots & h_{2,S} \\ \vdots & \vdots & \vdots & \vdots \\ h_{N,1} & h_{N,2} & \dots & h_{N,S} \end{bmatrix} \tag{3}$$

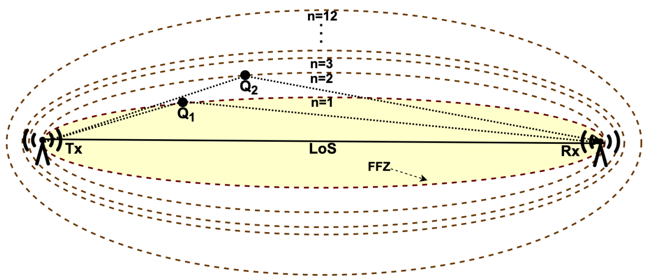

Fig. 1: The Fresnel zone reflection model

B. Fresnel Zone

Previous works verify the existence of the Fresnel zone model for human sensing in an indoor environment [20]. As shown in Fig. 1, Fresnel zones are concentric ellipses that take a pair of transceivers as foci. For simplicity, we also use Tx and Rx to represent the positions of transceivers and use $|T_xR_x|$ to represent the distance between them. With a given radio wavelength λ, the Fresnel zone can be constructed by (4), where n is the number of concentric ellipses and Q_n is a point in the n^{th} ellipse. When a person appears in the Fresnel zone at position Q_x, an additional signal path is generated due to the reflection of signals caused by the human body. When there are human motions, the path of reflected signals changes, leading to fluctuations in the signal amplitude. If there are more targets within the Fresnel zone, there will be more paths and more fluctuations in the amplitude of the signals.

$$|T_xQ_n| + |R_xQ_n| - |T_xR_x| = \frac{n\lambda}{2} \tag{4}$$

In the Fresnel Zone model, another issue that needs to be considered is the innermost ellipse, which is defined as the first Fresnel zone (FFZ). As more than 70% of the signal energy is transferred via the FFZ, diffracted signals are stronger than reflected signals, and dominate when the target moves inside the FFZ [21]. As a result, the Fresnel reflection model is unsuitable for targets within the FFZ, leading to an ineffective area (IA) for wireless sensing [19]. For targets inside and outside the FFZ, different models should be applied for CSI-based sensing. For passenger counting, we design a topology to make sure all passengers are located beyond the FFZ so that the Fresnel reflection model can be applied to the system.

$F_1 = \sqrt{(cD/f)}$ denotes the maximum diameter of the FFZ [22], where c is the light speed, D is the distance between the transceivers, and f is the radio frequency. Fig. 2 illustrates the deployment of our system in a bus compartment. When we put the access point (AP) and Rx at the front and rear of the upper deck of the bus (topology 1), the distance between the transceivers is around 10 m, i.e., with 5 GHz frequency, the maximum diameter of the FFZ is approximately 0.77 m. When we put the AP at the center and the two Rxs at the front and rear of the upper deck of the bus (topology 2), the distance between the transceivers is around 5 m, and the maximum diameter of the FFZ reduces to about 0.55 m, which is closer to

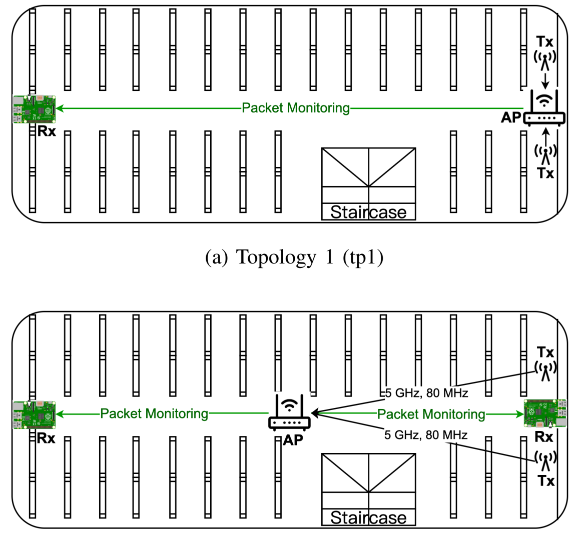

(a) Topology 1 (tp1)

(b) Topology 2 (tp2)

Fig. 2: Layout of the Bus Compartment

the width of the aisle (around 0.5 m). In that way, no passenger is located in the FFZ as they sit on both sides of the aisle.

III. System Design

A. CSI-enabled Wi-Fi Router Platform

The system designed for the bus compartment uses a passive collection method, i.e., A Tx communicates with an AP, while an Rx monitors the packets and collects CSI from them. The layouts for the two topologies, tp1 and tp2, are shown in Fig. 2, and the reason for having these deployments is explained in Section II-B. For this experiment, we used two extra Raspberry Pis as transmitters. In real scenarios, there is no need for an additional Tx since passengers will connect their phones or other Wi-Fi devices to the AP and generate enough communication packages in the ambient environment. This method reduces the requirement of hardware and power costs. It is also more cost-effective compared to an active collection method, like the Linux 802.11n CSI Tool [1], which needs the Tx to send signals to the Rx.

B. Data Preprocessing

CSI data collected using the Nexmon CSI Tool are quite noisy [23] and need further preprocessing. Since the phase is full of noise caused by the carrier frequency offset (CFO) and sampling frequency offset (SFO), we only employed the amplitude component of the received CSI in this system. To improve the performance, we removed 14 null subcarriers, resulting in 242 subcarriers for 80 MHz. The following two preprocessing steps are applied to the CSI data: 1) CSI calibration and 2) CSI feature extraction.

1) CSI Calibration: The original CSI extracted from the receiver is multiplied by a factor due to AGC. The AGC negatively affects CSI amplitude-based applications as it will distort the valuable features in the wireless signal. The scale of the CSI amplitude thus does not only depend on the distance between the Tx and Rx but also on changes in the environment and human movements. The amplitude of the CSI extracted after AGC is not able to provide accurate distance information according to the path-loss principle, and hence the sensing coverage of CSI amplitude-based solutions is limited to 2-4 m [24]. Since our system uses CSI amplitude data, reversing the AGC process and calibrating the original CSI amplitude is necessary. A calibration method based on the received signal strength (RSS) proposed by Gao et al. [25] is applied to improve the robustness of our system.

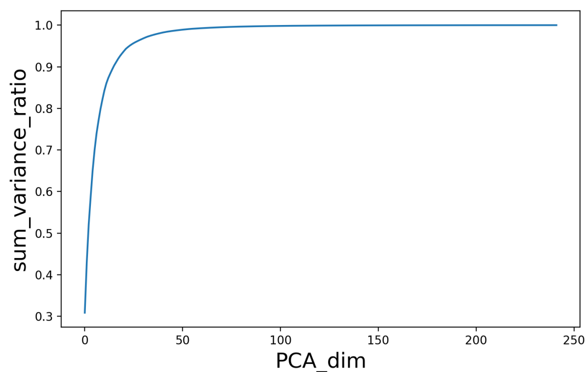

Fig. 3: Ratios of information remaining with PCA

2) CSI Feature Extraction: PCA is used to discover the correlations between CSI streams. The changes caused by body movements are correlated in all CSI subcarriers. More passengers will introduce more motions, i.e., more correlations between CSI streams. Based on this phenomenon, we use PCA to extract features for passenger counting. Wang et al. [26] pointed out that the 1st component of PCA is mainly noise and they extract characteristics from the 2nd and 3rd components. We figured out that removing the 1st component has a negative effect on the result. Authors in [27] also mentioned that there is more useful information than noise in the 1st component. To determine the suitable number of remaining components for further process, we calculate the ratio of information before and after PCA with a range from 0 to 242 dimensions and plot it in Fig. 3. When the dimension is 119, 99.9% of information is retained, which means the information loss is minimized. With this technique, the input size for one receiver can be reduced by about 50.83%. When we combine multiple receivers, it helps to reduce more dimensions. The calculation complexity and training time are reduced significantly with the same level of accuracy since useful information is maintained.

C. Machine Learning for Crowd Counting

Since this paper focuses on the improvement contributed by multiple sensors and the corresponding topologies, we use conventional machine learning techniques, including support vector machines (SVM), random forest (RF), and K-nearest neighbors (KNN), to train the passenger counting classifiers and compare the performance of different topologies. For topology 2, we concatenate the CSI data collected from the two receivers and use the PCA method to make sure that the input has the same size as the single receiver case. Although using deep learning methods and applying fusion methods like weighted sum or probability fusion will further improve the accuracy [28], this will be explored in our future work due to the space limit here.

The five-fold cross-validation method is utilized in this system. The CSI data is split into 5 subsets, and one of them is selected as the test data, while the remaining four datasets are used to train the model. After repeating this step for five times, the system performance is obtained by averaging all five results.

IV. Implementation and Evaluation

We used the Nexmon CSI Extraction Tool, which supports the low-cost Raspberry Pi platform [2]. This tool supports up to 80 MHz bandwidth with 802.11a/g/n/ac transmissions in both the 2.4 and 5 GHz bands. To maximize the available information, we used 80 MHz with 5 GHz bands, capturing 242 subcarriers (nulls removed). All CSI datagrams were saved in a pcap file that can be processed by Python or Matlab. We used Raspberry Pi 4B as receivers, and on each Rx, we configured channel 36 and filtered the transmitter with the nexutil command [2]. We used a Huawei WS7002 router as an AP since it is cheap and small enough to be installed in a bus compartment. Since the Raspberry Pi has one antenna and its Wi-Fi chip only has one core, each Pi will collect a single CSI matrix. We used 1000 Hz as the sampling frequency and collected CSI data from 0 to 20 passengers under scenarios with topology 1 and topology 2 on the same day.

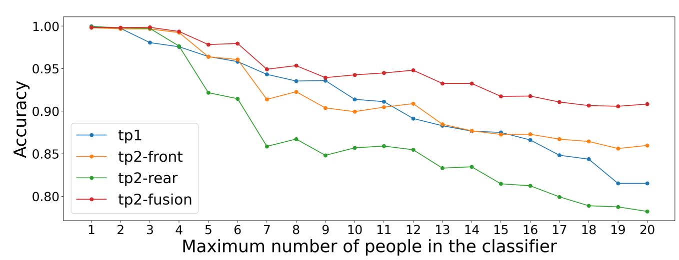

Fig. 4: Comparison of the accuracy between tp1 and tp2 for different number of classes with the SVM model

We used 30,000 samples for each class to train a model. We tried various kernel functions with SVM and figured out that the radial basis function (RBF) kernel is the most suitable one. The performance of using SVM with RBF kernel is shown in Fig. 4. For topology 1, the maximum number of passengers that can be classified with an accuracy above 90% is 11. For topology 2, when using the CSI extracted from one of the two receivers to train the model, it achieves up to 12 and 6 passengers with an accuracy higher than 90% for the Rx at the front and rear respectively. When combining the data collected from both receivers in topology 2, all 20 passengers can be classified with an average accuracy of 90.83%. One possible

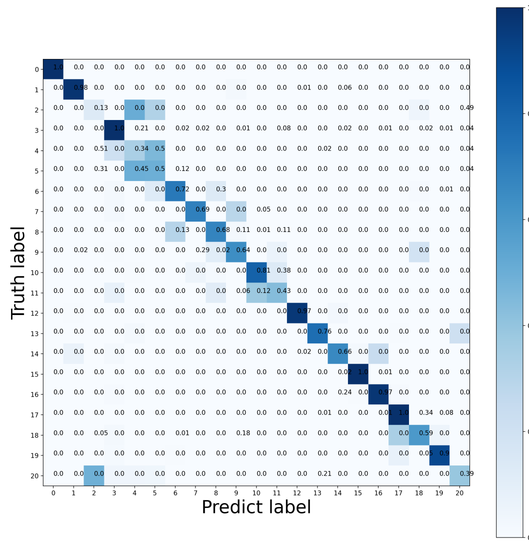

(a) Topology 1

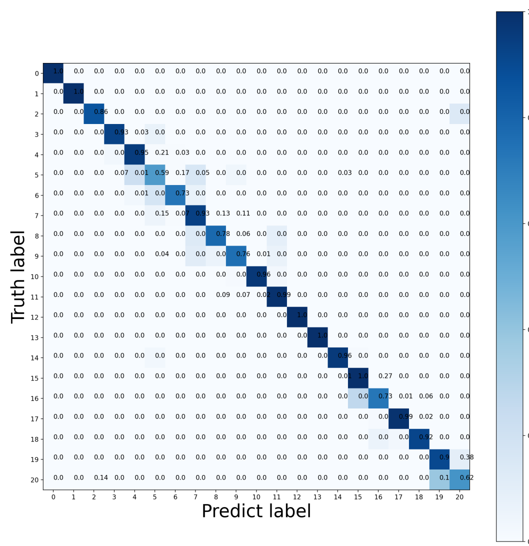

(b) Topology 2

Fig. 5: The confusion matrices for the SVM model with up to 20 passengers for (a) Topology 1 and (b) Topology 2.

reason for the different performance of the front and rear Rx is the hardware discrepancy. Although the type and specifications are the same (Raspberry Pi 4B, 8G), the manufacturing process is not ideal and exactly the same for all devices, leading to different quality of the collected data [29]. Since the layout of the bus compartment is asymmetric, it may also impact the path and noise of the signals. Denoising methods can be applied to reduce the difference caused by this issue.

TABLE I: Accuracy Results of Topologies with Various ML Methods

Models	tp1	tp2_front	tp2_rear	tp2_fusion	Improvement
SVM	81.46%	86.04%	78.22%	**90.83%**	11.49%
RF	79.34%	84.17%	75.37%	86.31%	8.79%
KNN	74.40%	81.20%	74.44%	87.97%	18.24%

Fig. 5 shows the confusion matrices for SVM with up to 20 passengers in the two topologies, which illustrates the classification distributions. As can be observed, there are generally more instances of misclassification for topology 1 than for topology 2, resulting in a lower average accuracy for topology 1, as shown in Table I. For tp2, the estimated number of passengers is only 0 or 1 off from the true number, while for tp1, it misclassifies the number of passengers with a larger error, like the two and 20 passengers cases shown in Fig. 5a. The mean absolute error (MAE) for the exact number of passengers with tp1 is 0.77, while it reduces to 0.20 with tp2. Since all other settings like the collection date and passengers' locations are the same for these two topologies, the classification distributions and the MAE metric illustrate that the designed topology improves the robustness of the passenger counting system. For up to 20 passengers, with all other settings the same as tp1, tp2 improves the counting accuracy by about 11.49%. To verify that this improvement is valid in general, RF and KNN methods are used to train the classifiers with the same dataset, and the comparison results are shown in Table I. We empirically set the number of estimators to 90 for the RF method and the number of neighbors to 10 for the KNN method. For these two methods, tp2 improves the accuracy by 8.79% and 18.24% respectively.

From this experiment, we figured out that with the same preprocessing and crowd-counting methods, increasing the number of receivers does improve the accuracy or the maximum number of people with acceptable accuracy. Most researchers focus on applying more complex techniques for signal processing and crowd counting to improve the accuracy or the sensing scalability. From another perspective, using multiple devices with a suitable topology can also improve the estimation accuracy with the same level of complexity or maximum number of people. The results in this paper will serve as a benchmark for future model training methods, such as deep learning. More advanced data processing and passenger counting techniques will further improve the accuracy of the given hardware and topology.

V. Conclusion

In this paper, we proposed a deployment scheme to improve the robustness and extend the scalability of the CSI-based crowd-counting system. To the best of our knowledge, this is the first work that considers the deployment of more than one receiver for Wi-Fi-based device-free stationary crowd counting. It considers the impact of the transmitter and receiver locations on the system performance and combines the Fresnel zone concept to design a suitable topology for passenger counting on a double-decker bus. We preprocessed the original signal by removing the effect of the automatic gain control and utilized the principal component analysis method to extract features from multiple receivers. A support vector machine model was trained to estimate the number of passengers on the upper deck of a bus. To verify the effectiveness of the proposed methodology in the crowd-counting system, we conducted experiments with two topologies and up to 20 passengers.

Our results show that the average accuracy of the proposed topology with two receivers is 90.83%, which outperforms the benchmark with a single receiver by 11.49%.

The work of this paper will lay the ground for our future work. We plan to further increase the maximum number of people supported by the counting system by designing optimal topologies or applying data fusion methods. In addition, we will evaluate the proposed deployment in various environments over a long period of time to validate the temporal robustness and adaptability of proposed CSI learning models.

REFERENCES

[1] D. Halperin, W. Hu, A. Sheth, and D. Wetherall, "Tool release: Gathering 802.11n traces with channel state information," *SIGCOMM Comput. Commun. Rev.*, vol. 41, no. 1, p. 53, jan 2011. [Online]. Available: https://doi.org/10.1145/1925861.1925870

[2] F. Gringoli, M. Schulz, J. Link, and M. Hollick, "Free your csi: A channel state information extraction platform for modern wi-fi chipsets," in *Proceedings of the 13th International Workshop on Wireless Network Testbeds, Experimental Evaluation & Characterization*, 2019, pp. 21–28.

[3] J. Filipic, M. Biagini, I. Mas, C. D. Pose, J. I. Giribet, and D. R. Parisi, "People counting using visible and infrared images," *Neurocomputing*, vol. 450, pp. 25–32, 2021.

[4] S. Zhang, Y. Wu, C. Men, and X. Li, "Tiny yolo optimization oriented bus passenger object detection," *Chinese Journal of Electronics*, vol. 29, no. 1, pp. 132–138, 2020.

[5] U. Mehmood, I. Moser, P. P. Jayaraman, and A. Banerjee, "Occupancy estimation using wifi: A case study for counting passengers on busses," in *2019 IEEE 5th World Forum on Internet of Things (WF-IoT)*. IEEE, 2019, pp. 165–170.

[6] J.-H. Choi, J.-E. Kim, and K.-T. Kim, "People counting using ir-uwb radar sensor in a wide area," *IEEE Internet of Things Journal*, vol. 8, no. 7, pp. 5806–5821, 2020.

[7] S. T. Kouyoumdjieva, P. Danielis, and G. Karlsson, "Survey of non-image-based approaches for counting people," *IEEE Communications Surveys & Tutorials*, vol. 22, no. 2, pp. 1305–1336, 2020.

[8] H. Hou, S. Bi, L. Zheng, X. Lin, Y. Wu, and Z. Quan, "Dasecount: Domain-agnostic sample-efficient wireless indoor crowd counting via few-shot learning," *IEEE Internet of Things Journal*, vol. 10, no. 8, pp. 7038–7050, 2022.

[9] S. Liu, Y. Zhao, F. Xue, B. Chen, and X. Chen, "Deepcount: Crowd counting with wifi via deep learning," *arXiv preprint arXiv:1903.05316*, 2019.

[10] R. F. Brena, E. Escudero, C. Vargas-Rosales, C. E. Galvan-Tejada, and D. Munoz, "Device-free crowd counting using multi-link wi-fi csi descriptors in doppler spectrum," *Electronics*, vol. 10, no. 3, p. 315, 2021.

[11] H. Choi, M. Fujimoto, T. Matsui, S. Misaki, and K. Yasumoto, "Wi-cal: Wifi sensing and machine learning based device-free crowd counting and localization," *IEEE Access*, vol. 10, pp. 24 395–24 410, 2022.

[12] H. Zou, Y. Zhou, J. Yang, W. Gu, L. Xie, and C. Spanos, "Freecount: Device-free crowd counting with commodity wifi," in *GLOBECOM 2017-2017 IEEE Global Communications Conference*. IEEE, 2017, pp. 1–6.

[13] Z. Guo, F. Xiao, B. Sheng, L. Sun, and S. Yu, "Twcc: a robust through-the-wall crowd counting system using ambient wifi signals," *IEEE Transactions on Vehicular Technology*, vol. 71, no. 4, pp. 4198–4211, 2022.

[14] F. Wang, F. Zhang, C. Wu, B. Wang, and K. R. Liu, "Respiration tracking for people counting and recognition," *IEEE Internet of Things Journal*, vol. 7, no. 6, pp. 5233–5245, 2020.

[15] Y.-K. Cheng and R. Y. Chang, "Device-free indoor people counting using wi-fi channel state information for internet of things," in *GLOBECOM 2017-2017 IEEE Global Communications Conference*. IEEE, 2017, pp. 1–6.

[16] H. Jiang, S. Chen, Z. Xiao, J. Hu, J. Liu, and S. Dustdar, "Pa-count: Passenger counting in vehicles using wi-fi signals," *IEEE Transactions on Mobile Computing*, 2023.

[17] B. Korany and Y. Mostofi, "Counting a stationary crowd using off-the-shelf wifi," in *Proceedings of the 19th Annual International Conference on Mobile Systems, Applications, and Services*, 2021, pp. 202–214.

[18] X. Wang, K. Niu, J. Xiong, B. Qian, Z. Yao, T. Lou, and D. Zhang, "Placement matters: Understanding the effects of device placement for wifi sensing," *Proceedings of the ACM on Interactive, Mobile, Wearable and Ubiquitous Technologies*, vol. 6, no. 1, pp. 1–25, 2022.

[19] F. Wang, W. Gong, and J. Liu, "On spatial diversity in wifi-based human activity recognition: A deep learning-based approach," *IEEE Internet of Things Journal*, vol. 6, no. 2, pp. 2035–2047, 2018.

[20] H. Wang, D. Zhang, J. Ma, Y. Wang, Y. Wang, D. Wu, T. Gu, and B. Xie, "Human respiration detection with commodity wifi devices: Do user location and body orientation matter?" in *Proceedings of the 2016 ACM international joint conference on pervasive and ubiquitous computing*, 2016, pp. 25–36.

[21] F. Zhang, K. Niu, J. Xiong, B. Jin, T. Gu, Y. Jiang, and D. Zhang, "Towards a diffraction-based sensing approach on human activity recognition," *Proceedings of the ACM on Interactive, Mobile, Wearable and Ubiquitous Technologies*, vol. 3, no. 1, pp. 1–25, 2019.

[22] A. F. Molisch, *Wireless communications*. John Wiley & Sons, 2012, vol. 34.

[23] J. Schäfer, B. R. Barrsiwal, M. Kokhkharova, H. Adil, and J. Liebehenschel, "Human activity recognition using csi information with nexmon," *Applied Sciences*, vol. 11, no. 19, p. 8860, 2021.

[24] Y. Li, D. Wu, J. Zhang, X. Xu, Y. Xie, T. Gu, and D. Zhang, "Diversense: Maximizing wi-fi sensing range leveraging signal diversity," *Proceedings of the ACM on Interactive, Mobile, Wearable and Ubiquitous Technologies*, vol. 6, no. 2, pp. 1–28, 2022.

[25] Z. Gao, Y. Gao, S. Wang, D. Li, and Y. Xu, "Crisloc: Reconstructable csi fingerprinting for indoor smartphone localization," *IEEE Internet of Things Journal*, vol. 8, no. 5, pp. 3422–3437, 2020.

[26] W. Wang, A. X. Liu, M. Shahzad, K. Ling, and S. Lu, "Understanding and modeling of wifi signal based human activity recognition," in *Proceedings of the 21st annual international conference on mobile computing and networking*, 2015, pp. 65–76.

[27] X. Yang, S. Wu, M. Zhou, L. Xie, J. Wang, and W. He, "Indoor through-the-wall passive human target detection with wifi," in *2019 IEEE Globecom Workshops (GC Wkshps)*. IEEE, 2019, pp. 1–6.

[28] W. Wang, A. X. Liu, M. Shahzad, K. Ling, and S. Lu, "Device-free human activity recognition using commercial wifi devices," *IEEE Journal on Selected Areas in Communications*, vol. 35, no. 5, pp. 1118–1131, 2017.

[29] C. Li, Y. Jiang, and A. Hu, "Csi measurement and reciprocity evaluation method based on embedded platform," in *2021 IEEE 94th Vehicular Technology Conference (VTC2021-Fall)*. IEEE, 2021, pp. 1–6.